International Journal of Modern Engineering Research (IJMER)
www.ijmer.com Vol.2, Issue.5, Sep-Oct. 2012 pp-3829-3834 ISSN: 2249-6645

Optical Absorption and Fluorescence Spectral Analysis of Nd^{3+} Doped Bismuth Boro-Silicate Glasses

Sunil Bhardwaj[a], Rajni Shukla[a], Sujata Sanghi[b], Ashish Agarwal[b], Inder Pal[b]
[a]*Department of Physics, Deenbandhu Chhotu Ram University of Science and Technology, Murthal, Sonipat-131093, Haryana, India*
[b]*Department of Applied Physics, Guru Jambheshwar University of Science and Technology, Hisar-125001, Haryana, India*

Abstract: *Glasses having compositions $20B_2O_3.(79.5\text{-}x)Bi_2O_3.xSiO_2$ ($10 \le x \le 40$, mol%) doped with 0.5 mol% of Nd^{3+} ions were prepared by melt quench technique. The amorphous nature of the glasses was confirmed by X-ray diffraction studies. The spectroscopic properties of Nd^{3+} ions in borate bismuth silicate glasses as a function of bismuth oxide were investigated using optical absorption and fluorescence spectra. The Judd-Ofelt theory has been employed to calculate transitions probability from the data of absorption cross-section of several f-f transitions. The intensity parameters Ω_2, Ω_4, and Ω_6 are determined by applying least square analysis method. The variation of Ω_2 and Ω_6 with Bi_2O_3 content has been attributed to changes in the asymmetry of the ligand field at the rare earth ion site and to the changes in the rare earth oxygen (RE-O) covalency. The variation of Ω_4 with Bi_2O_3 content has been attributed to rigidity of the samples. Using the Judd Ofelt intensity parameters the other radiative properties like radiative transition probability, radiative life time, branching ratio and the stimulated emission cross-sections of prepared BBSN glasses have been calculated. The main fluorescence transition $^4F_{3/2} \rightarrow {}^4I_{11/2}$ of Nd^{3+} ion has been investigated as a function of Bi_2O_3 in host glass.*

Keywords: *Fluorescence properties, Heavy metal oxides, Judd-Ofelt theory, Optical properties, Rare earth ions*

I. INTRODUCTION

In recent decades an increasing interest in rare earth doped glasses from the viewpoint of their spectroscopic properties and technological applications in many fields is observed. In fact, they are suitable materials for photonic devices such as planar optical waveguides, optical fiber amplifiers, wave guide laser etc [1-3]. Ever since the first solid state laser was demonstrated in 1961 by Snitzer in Nd^{3+} doped glasses, a lot of efforts are being done for the development of laser glasses. Neodymium doped glasses have attracted attention as they act as key element for optical amplifier around 1.3 μm and for higher power laser applications around 1.05 μm [4]. The outer shell configuration of neodymium is $4f^{12}\,5s^2\,5p^6\,6s^2$. The transition probability between 4f states, however are sensitive to the ions surrounding the rare earth ions.

In general, the optical and spectroscopic properties of rare earth ions are strongly dependent on host materials. The host glass materials should have high refractive index with good chemical and thermal stability along with low melting temperature of heavy metals in order to become more practically useful industries. Many potential host materials for rare earth ions have been developed [5]. One of the preferred host materials is oxide glasses which are chemically durable, thermally stable, optically transparent at the excitation and lasing wavelengths [6].Glasses based on heavy metal oxides (such as Bi_2O_3) have received increased attention due to their manifold possible applications in the field of glass ceramics, layers for optical, optoelectronics devices, thermal and mechanical sensors, reflecting windows etc [7]. The large polarizability of bismuth makes it suitable for possible non linear optical devices and environmental guide lines [8]. Wide transmitting window in the optical region having sharp cut-off in both UV-VIS and IR region make these glasses useful in spectral devices [9].

Further, Judd-Offelt theory has been employed to calculate the intensities of f-f transition in the absorption spectra of the rare earth ion. Experimental investigations of absorption spectra of rare earth ions in different matrices have revealed that the oscillator strengths for the specific transitions of rare earth ions depend more strongly on the structural features of materials and on the chemical nature of the ligands surrounding the rare earth ion as compared to other transitions. Once the experimental values of the oscillator strengths are determined from the integrated absorption coefficient, the intensity parameters can be obtained. When the phenomenological parameters Ω_λ are calculated, it is possible to derive the strength of any absorption or emission transition, as well as the stimulated emission cross-section and fluorescence branching ratio. Such spectral studies give valuable information about the structure and bonding in glass and radiative and non radiative properties of rare earth ions doped in glass matrix. This information is essentially required while developing new optical devices [10].

II. Theoretical details

Judd-Ofelt [11-12] theory has been used to investigate radiative nature of trivalent rare earth ions in a variety of laser host materials. The intensity parameter, radiative life time, and branching ratio are calculated with refractive index using Judd-Ofelt analysis. The experimental oscillator strength was calculated from the absorption spectra by using the equation.

$$f_{\text{meas.}} = 4.32\times10^{-9} \int \varepsilon(\upsilon) d\upsilon \qquad (1)$$

where ε (ν) is the molar absorptivity (cm^2) of absorption band at energy υ(cm^{-1}).The experimental oscillator strengths were used to obtained values of the intensity parameters (λ = 2, 4, 6) following the standard least square fitting method. The validity of the fitting is examined by comparing the experimental and theoretical oscillator strengths. The Judd-Ofelt intensity parameters (Ω_λ) are phenomenological characteristics for the influence of surrounding environment of the rare earth ions as they contain implicitly the crystal field terms and the radial wave function. According to the Judd-Ofelt theory the oscillator strength for an electronic transition from the initial manifold (SL, J) to the final manifold (S'L', J') is given by the expression.

$$f_{cal} == \frac{8\pi^2 mc}{3h(2j+1)\lambda_p}\left(\frac{(n^2+2)^2 S_{ed}}{9n}\right) \quad (2)$$

Where c represents the velocity of light, n represent refractive index, λ_p represent the absorption peak wavelength, e and m the electron charge and mass, S_{ed} represents the line strengths for the induced electric dipole transition, which is given by:

$$S_{ed} = \sum_{t=2,4,6} \Omega_t \left| \left\langle SLJ \| U^t \| S'L'J' \right\rangle \right|^2 \quad (3)$$

The spontaneous emission probability for the radiative decay, Arad (sec-1), from the initial manifold (SLJ) to the final manifold (S'L'J') is given by the expression.

$$A_{rad} = \frac{64\pi^4 e^2 \bar{\nu}^3 n(n^2+2)^2}{3h(2j+1)9} \times S_{ed} \quad (4)$$

Where $U^{(\lambda)}$ (λ=2, 4, 6) are the matrix elements of unit tensor operators and had been calculated by Carnall et al. The total probability, A_T, obtained by carrying out the summation of all the transitions to the final state bj' is given by

$$A_T = \sum A_{rad} \quad (5)$$

The fluorescence branching ratio is given by

$$\beta_r = \frac{A_{rad}}{A_T} \quad (6)$$

The radiative life time is represented by

$$\tau_r = \frac{1}{A_T} \quad (7)$$

The induced emission cross-section for each transition could be estimated from the emission spectra by [9].

$$\sigma = \frac{\lambda_p^4 A_{rad}}{8\pi c n^2 \Delta\lambda} \quad (8)$$

Where λ_p is peak wavelength and $\Delta\lambda$ is the full width at half maxima of the fluorescent peak for different transitions obtained from emission spectra.

III. Experimental

Glasses having compositions $20B_2O_3.(79.5-x)Bi_2O_3.xSiO_2$ ($10 \le x \le 40$, mol%) doped with 0.5 mol% of Nd^{3+} ions were prepared by melt quench technique. Appropriate amount of AR grade chemicals (B_2O_3, Bi_2O_3, SiO_2 and Nd_2O_3) having purity above 99.99% were weighed on 0.001% accuracy and mixed thoroughly. The raw mixed materials were melted in a muffle furnace in air (at 1150 ^{0}C for 40 min). The crucible was shaken frequently after every 10 minutes for the homogeneous mixing of all the constituents. The melt was quenched at room temperature by pouring between two stainless steel plates. The quenched samples were annealed to minimize the internal strain and then allowed to cool slowly to room temperature. The exact composition along with the codes of the samples is given in Table 1 .The samples were polished for spectral and other investigations. The amorphous nature of the glasses was confirmed by recording the X-ray diffraction pattern using Mini Flex Desktop X-ray Difractometer with Cu-Kα line of wavelength at the scanning rate of 2^0/min and 2θ was varied from 10^0 to 80^0.

The refractive index (n) of the prepared samples was measured by the Brewster angle method using He-Ne laser (633 nm). The density (D_g) of all the glasses were measured by using Archimedes principle with xylene as immersing liquid. The relation used is

$$D_g\left(gm/cm^3\right) = \frac{W_a}{W_a - W_b} D_x \quad (9)$$

Where W_a is the weight of glass sample in air, W_b is the weight of glass sample when immersed in xylene and D_x is the density of xylene (0.86 gm/cm^3).

The Optical absorption spectra of all the polished samples were recorded on a Varian-Carry 5000 spectrophotometer in the range 300-3200 nm. The emission spectra were recorded using Fluoro-max-3 Fluorimeter with Xe arc lamp as the excitation source at wavelength of 800 nm.

IV. RESULT AND DISCUSSION

4.1 Physical parameters

Various physical properties of all glasses as a function of Bi_2O_3 content were determined from the experimental data and are listed in Table 1. It is clearly observed that density decrease monotonously when Bi_2O_3 is replaced by SiO_2 in the glass. This may be due to greater molar mass of Bi_2O_3 (438.96) than that of SiO_2 (60.08). The decrease in molar volume on the other hand shows that addition of SiO_2 may contract the structure of the loose network in the studied glass. Also the smaller values of radii and bond length of SiO_2 than that of Bi_2O_3 results in decrease in the volume of these glasses

During recent years the optical basicity has been suceesfully used to correlate a range of properties of glass with chemical composition. The optical basicity of a material can be experimentally determined using UV probe ion spectroscopy. It was found that the frequency of the UV absorption band shifts gradually with composition. The

optical basicity (Λ) addresses the ability of oxide glass in contributing the negative charges in the glass matrix. In other words it defines the electron donating power of the oxygen in the oxides glass. The theoretical optical basicity can be calculated by the equation proposed by Duffy and Ingram

$\Lambda_{th} = X_1\Lambda_1 + X_2\Lambda_2 + X_3\Lambda_3 + \ldots\ldots + X_n\Lambda_n$ (10)

Where X_1, X_2, ……X_n are equivalent fraction based on the amount of oxygen each oxide contributes to the overall glass stoichometry and Λ_1, Λ_2, Λ_3 ……Λ_n are basicities assigned to the individual oxides.

The optical basicity of Bi_2O_3 is higher than that of SiO_2 therefore basicity decreases with decrease of Bi_2O_3 in the host glass.

Electronic polarizability, α, has important chemical implications and has been the subject of several studies. It can be obtained experimentally from refractivity measurements using the lorentz-lorentz relationship.

$$\alpha_m = \frac{3R_m}{4\Pi N} \quad (11)$$

Where N is Avogadro's number and the molar electronic polarizability is measured in $Å^3$.It is well known that Bi^{3+} cation posses a very high polarizability (1.508 A^{o3}), which is due to their large ionic radii and small cation unit field strength. Moreover, Bi^{3+} ions possess a lone pair in the valence shell This relation presents a general tendency toward an increase in the oxide polarizability with increasing optical basicity.

The refractive index (n) depends on individual ions present in the glass and polarizability of cations. In general, the refractive index of the glass increases for the highly polarizable cations as a result of increase in the non-bridging oxygen to bridging oxygen ratio [13]. It was established by Dimitrov and Saka that there is a general trend by which refractive index increases with the increase in electronic polarizability of oxide ions.Since in the present sample the basicity decreases, which results in the decrease of electronic polarizability, therefore the refractive index also decreases upon the replacement of bismuth with silicate in the glass network. A good agreement is observed between theoretical and observed values as shown in Table.1.

The molar refraction is considered as the sum of the contributions of the cationic refraction and oxygen ionic refraction. It is related to the structure of the glass which measures the bonding condition in the glass [14]. The molar refraction (R_m) derived by Lorentz and Lorentz relationship.

$$R_m = \left[\frac{n^2-1}{n^2+2}\right]V_m \quad (12)$$

Where the quantity $(n^2-1)/(n^2+2)$ is called the reflection loss and V_m is the molar volume in cm^3.

Accoding to duffy [20] the energy gap is given as

$$E_g = 20\left(1-\frac{R_m}{V_m}\right)^2 \quad (13)$$

As the value of n decreases, there is decrease in the value of R_m/V_m due to which Eg increases.If energy gap is large, λ_p will be small and hence σ decreases.

The optical basicity of an oxidic medium is the average electron donar power of all the oxide atoms comprising the medium. Increasing basicity results in increasing negative charge on the oxygen atom and thus, increasing covalency in the cation- oxygen bonding.

Fig. 1 presents the X-ray diffraction pattern of BBSN-1 with Cu-Kα (15.42 nm) line of wavelength at the scanning rate of 2^0/min and 2θ was varied from 10^0 to 80^0. The XRD pattern of glass exhibits broad hump, which shows its amorphous nature.

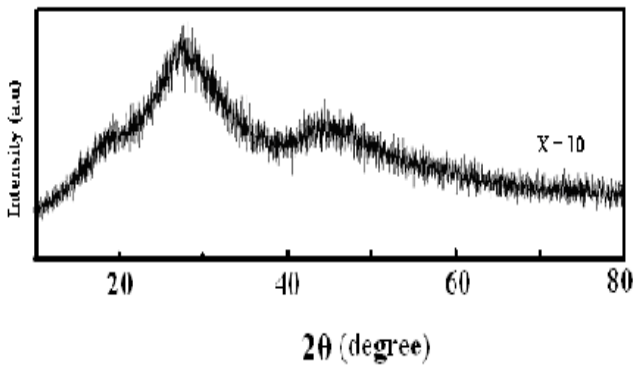

Fig.1. X-ray diffraction pattern of BBSN-1

Table1: Density (D), molar volume (V_m), refractive index (n), reflection loss (R_L), molar refraction (R_m),electronic polarizability (α_m), energy gap (E_g) and optical basicity (Λ) of $20B_2O_3$.(79.5-x) Bi_2O_3.xSiO_2 0.5 Nd_2O_3 ($10 \le x \le 40$) glasses.

Sample code	x (mol%)	D (g/cm^3)	V_m (cm^3/mol)	n	R_L (n^2-1/n^2+2)	R_m (cm^3 /mol)	α_m (A^o)^3	E_g (ev)	Λ
BBSN1	10	6.92	55.64	1.96	0.486	27.06	10.73	5.28	0.425
BBSN2	20	6.83	49.71	1.87	0.454	22.58	8.95	5.96	0.407
BBSN3	30	6.77	44.00	1.79	0.423	18.59	7.37	6.66	0.387
BBSN4	40	6.64	38.00	1.72	0.395	15.00	5.94	7.32	0.372

Table2:

Oscillator strength for some transitions from the indicated level to the ground level $^6H_{5/2}$, their root mean square (δ_{RMS}) Judd-Ofelt intensity parameters (Ω_2, Ω_4, Ω_6) of various Nd^{3+} doped BBSN glasses.

Transitions from $^6H_{5/2} \rightarrow$	λ(nm)	Oscillator strength (10^{-6})							
		BBSN1		BBSN2		BBSN3		BBSN4	
		f_{expt}	f_{cal}	f_{expt}	f_{cal}	f_{expt}	f_{cal}	f_{expt}	f_{cal}
$^4G_{9/2}$	514	1.85	1.96	1.35	1.02	1.22	1.24	1.14	1.12
$^4G_{7/2}$	526	3.85	4.32	6.77	5.92	5.35	4.77	5.03	5.23
$^4G_{5/2}$, $^2G_{7/2}$	586	5.53	5.20	4.23	5.10	3.22	3.82	2.35	2.13
$^4F_{9/2}$	684	2.99	3.19	1.03	1.07	1.01	0.69	1.06	1.16
$^4S_{3/2}$, $^4F_{7/2}$	750	2.45	2.43	3.53	3.62	3.45	3.51	3.31	3.56
$^4F_{5/2}$, $^2H_{9/2}$	798	2.37	2.23	3.45	3.22	3.16	3.09	3.28	3.34
δ_{RMS} (10^{-6})		5.07		4.64		3.97		3.69	
Ω_2(10^{-20}cm^2)		3.52		3.22		2.74		2.40	
Ω_4(10^{-20}cm^2)		4.19		5.05		5.54		5.59	
Ω_6(10^{-20}cm^2)		3.86		4.94		5.05		5.07	
Ω_4/Ω_6		1.01		1.02		1.09		1.10	

Table 3:

The peak wavelength (λ_p), radiative transition probability (A_{rad}), branching ratio (β_r), stimulated emission cross-section (σ), total radiative transition probability (A_T) and the radiative life time (τ_r) of Nd^{3+} ion doped BBSN glasses.

Transitions		**BBSN1**			**BBSN2**			**BBSN3**			**BBSN4**		
from $^4F_{3/2}$	λ_p (nm)	A_{rad} (s^{-1})	β_r (%)	σ (10^{-20}cm^2)	A_{rad} (s^{-1})	β_r (%)	σ (10^{-20}cm^2)	A_{rad} (s^{-1})	β_r (%)	σ (10^{-20}cm^2)	A_{rad} (s^{-1})	β_r (%)	σ (10^{-20}cm^2)
$^4I_{11/2}$	1075	1130	0.536	2.20	1023	0.545	2.03	946	0.543	1.88	789	0.570	1.69
$^4I_{9/2}$	905	980	0.464	1.67	854	0.454	1.44	746	0.428	1.07	595	0.430	0.91
A_T(s^{-1})		2110			1877			1742			1384		
τ_r(μs)		0.474			0.532			0.574			0.722		

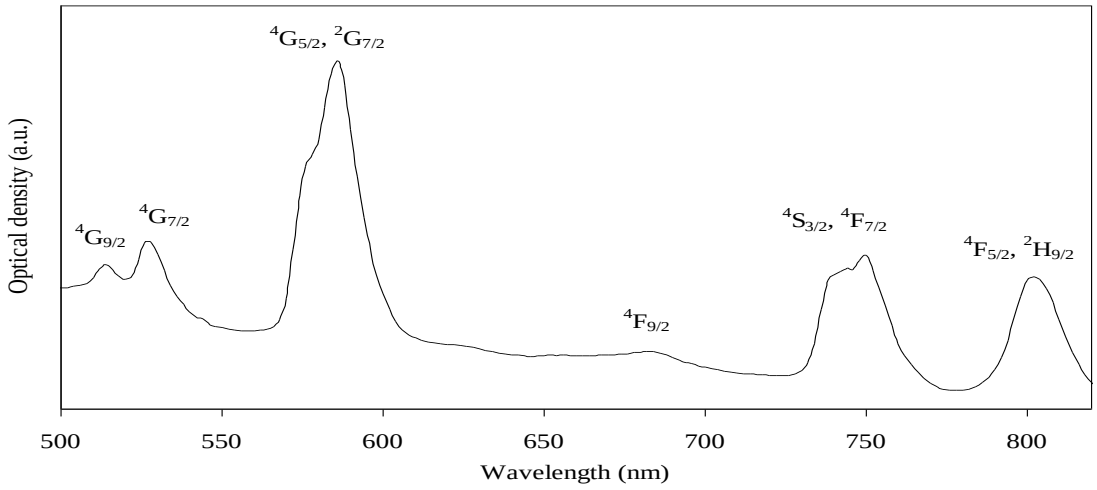

Fig. 2. Absorption spectrum of $20B_2O_3$ $69.5Bi_2O_3$ $10SiO_2$ $0.5\ Nd_2O_3$. (BBSN-1) glass sample.

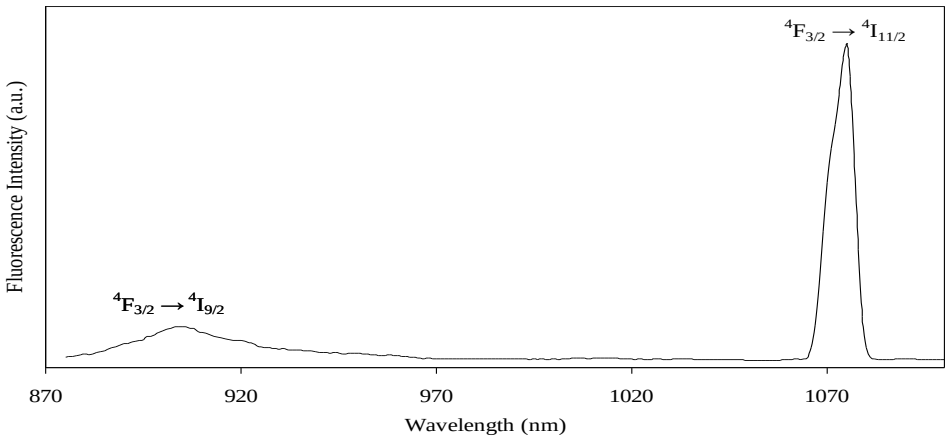

Fig. 3. Emission spectra of $20B_2O_3$ $69.5Bi_2O_3$ $10SiO_2$ 0.5 Nd_2O_3 (BBSN-1) glass sample.

4.2 Absorption spectra analysis

The optical absorption spectrum of BBSN-1 glass sample in the wavelength range 500-850 nm is shown in Fig.2. The absorption spectra for all other samples are qualitatively similar. From Fig. 2, the absorption bands at 514, 528, 586, 684, 750, 802 nm are observed, which predict the Nd^{3+} ion transitions from the ground state $^4I_{9/2}$ to various excited state within the 4f shell and are assigned as $^4I_{9/2} \rightarrow {}^4G_{9/2}$, $^4G_{7/2}$, $^4G_{5/2}+{}^2G_{7/2}$, $^4F_{9/2}$, $^4S_{3/2}$, $^4F_{5/2}+{}^2H_{9/2}$, respectively. It is worth noting that the transition $^4I_{9/2} \rightarrow {}^4G_{5/2}+{}^2G_{7/2}$ is the most intense than other transitions.

The values of oscillator strength obtained from experimental spectra and those calculated using the Judd-Ofelt parameters are given in Table 2 along with the respective root mean square (δ_{RMS}) deviations. From Table 2 it is observed that with the addition of SiO_2 in the host glasses the values of f_{expt}, f_{cal} and δ_{RMS} decreases. According to the Judd-Ofelt theory [11-12], the effect of the crystal field can be described by three intensity parameters Ω_λ (λ= 2, 4, 6). The intensity parameters are obtained from the experimental oscillator strengths and the calculated double reduced matrix elements by using least square analysis method [15].

The matrix elements used in the fitting procedure were those given by Carnall et al. [16]. The intensity parameters determined for Nd^{3+} ions doped glasses are listed in Table 3. The intensity parameters are found to be in the order $\Omega_4 > \Omega_6 > \Omega_2$ for all the glass samples. These intensity parameters reflect the local structure and bonding in the vicinity of rare earth ion to some extent. The parameter Ω_2 is associated with asymmetry of the ligand field near the rare earth ion so its value is expected to be higher when the symmetry of the ligand field at the rare earth site is lower. The decrease of Ω_2 with decrease in Bi_2O_3 content for Nd^{3+} ions indicate that the rare earth ion in lead bismuth silicate glasses might be surrounded by bismuthate groups that affect the symmetry of ligand field at the rare earth ion site.

The intensity parameter Ω_6 is related to covalency of RE-O bond and decreases with increasing covalency where as covalency of the RE-O bond is assumed to be related with the local basicity around the rare earth sites [17]. The optical basicity of Bi_2O_3 is higher than that of SiO_2, Therefore with decrease in Bi_2O_3 content in the host glass, covalency of Nd-O bond increases which results in the decrease in Ω_6 values. As a general conclusion, Ω_2 and Ω_6 parameters decrease with the increase in the degree of covalency of the rare earth oxygen bonds.

The intensity parameter Ω_4 is related to the rigidity of the host glass [18]. In the present glass samples the rigidity of the host glass decreases with the decrease in Bi_2O_3 content (Table3), similar results were reported earlier in Er^{3+} ion doped zinc bismuth borate glass [19].

4.3Fluorescence spectra analysis

Besides the main emission, near 1060 nm ($^4F_{3/2} \rightarrow {}^4I_{11/2}$) another transition at 905 nm ($^4F_{3/2} \rightarrow {}^4I_{9/2}$) is observed at λ_{ext} = 800 nm as shown in Fig.3. The ratio Ω_4 / Ω_6 which is usually considered as the spectroscopic quality factor (SQF) can be used to describe the strength of the emission transitions. The emission cross-section is expected to increase with increasing refractive index of a glass host, because the emission cross-section that is due to the electric dipole transitions of rare earth ions increases as the refractive index of the glass host [$\sigma_e \sim (n^2+2)/n$] increases.

For laser applications, the value of emission cross-section is an important parameter and signifies the rate of energy extraction from the optical material. A large stimulated emission cross-section is of benefit for a low threshold and a high gain in laser operation [20]. The effective bandwidth of the emission spectra is mainly caused by splitting of the levels of transitions and the site to site variation of the ligand field around Nd^{3+} ions in the glass i.e., inhomogeneous broadening. The slight decrease in effective bandwidth implies that the asymmetry of the ligand field becomes weaker. This result is again in accordance with decrease in the value of Ω_2 with Bi_2O_3 content in the host glass. From Table 3, it is observed that the stimulated emission cross-section (σ_e) and fluorescence intensity decrease with the decrease in Bi_2O_3 content in the host glass. These variations are in agreement with previous investigations. The high values of stimulated emission cross-section suggest that the prepared

glasses are potential candidates for the lasing host materials and for low threshold, high gain applications.

V. CONCLUSIONS

The refractive index of the glass reduces from 1.96 to 1.72 with the decrease in Bi_2O_3 / SiO_2 ratio. The spectroscopic properties of Nd^{3+} ions doped glasses have been analyzed on the basis of Judd-Ofelt theory. The intensity parameter Ω_2 is most sensitive to the local environment of Nd^{3+} ions, larger values (Ω_2 >2) suggest a less Centro symmetric coordination environment. The branching ratio for the $^4F_{3/2} \rightarrow {}^4I_{11/2}$ transition in the present glass is 57% and the predicted spontaneous radiative transition rate is as high as 2110 s^{-1} for BBSN1 sample. The stimulated emission cross-section for the $^4F_{3/2} \rightarrow {}^4I_{11/2}$ transition decreases from 2.20×10^{-20} to 1.69×10^{-20} cm^2, and it is comparable to the some of frequently used laser glasses. The results of these investigations indicate that neodymium doped bismuth boro-silicate glasses may be suitable host for the lasing materials. The IR absorbance analysis of these glasses confirmed the decrease in both the NBOs and the molar volume, which in turn explain the obtained decrease in the refractive indices, the polarizability, and the optical basicity of the studied glasses. Also, the observed decrease in the optical band gap is related to the weaker bond strength of the Bi-O compared to the Si-O.

REFRENCES

[1] A.A. Kamniskii Laser crystals. second ed. Springer, Berlin (1990), pp. 252-253

[2] E. Pacoraro, J.A. Sampaio, L.A.O. Nunes, S Gama and M.L. Baesso. Spectroscopic properties of Water free Nd_2O_3 Doped Low Silica Aluminosilcate Glass. Non-Cryst. Solids 77(2000)[3]B. Karthikeyan, R. Philip, S. Mohan. Optical and Non-linear Optical Properties of Nd^{3+} doped Heavy Metal Borate Glasses. Optics Commun 246 (2005) 153.

[4] Boehm L., Reisfeld R., Sepctor N., Optical transitions of Sm^{3+} in oxide glasses, Journal of Solid State Chemistry, 28 (1979) 75.

[5] Stone B.T., Bray K.L., Fluorescence properties of Er^{3+}-doped sol-gel glasses, Journal of Non-Crystalline Solids, 197 (1996) 136.

[6] Reisfeld R., Jorgensen C.K., Lasers and Excited States of Rare Earths, Springer, Berlin, (1977).

[7] Ratnakaram Y.C., Thirpathi N.D., Chakaradhar R.P.S., Spectral studies of Sm^{3+} and Dy^{3+} doped lithium cesium mixed alkali borate glasses, Journal of Non-Crystalline Solids, 352 (2006) 3914.

[8] Jiangting Sun, Jihua Zhang, Baojiu Chen et al. Preparation and optical properties of Er^{3+} doped gadolinium borosilicate glasses. Journal of Rare Earths 23(2) (2005) 157.

[9] I. Operea, H. Hesse, K. Betzler. Optical properties of bismuth borate glasses. Optical Materials 26(3) (2004) 235.

[10] P. Becker. Thermal and Optical Properties of Glasses of the System Bi_2O_3-B_2O_3 Cryst. Res. Technol. 1 (2003) 74

[11] B.R. Judd. Optical Absorption Intensities of Rare-Earth Ions. Phy. Rev. 127 (1962) 750.

[12] J.S. Ofelt. Intensities of Crystal Spectra of Rare-Earth Ions. Chem Phys, 37 (1962) 511.

[13] X. Zou, T. Izumitani Spectroscopic properties and mechanisms of excited state absorption and energy transfer upconversion for Er^{3+} doped glasses. J. Non-Cryst. Solids 162 (1) (1993) 68.

[14] S. Tanabe, T Ohayagi and N Soga, et al. Compositional dependence of Judd-Ofelt parameters of Er^{3+} ions in alkali metal borate glass. Phys. Rev. B46 (1992) 3305.

[15] W.F. Krupke, Induced-emission cross-section in neodymium laser glasses. IEEE J. Quantum electron QE-10 (1974) 450-457

[16] W.T. Carnall, P.R. Fdcids, K. Rajnax. Electronic energy levels in the trivalent lanthanide aquo ions. The journals of Chemical Physics 49(10) (1968) 4424.

[17] A. Agarwal, I. Pal, S. Sanghi, M.P. Aggarwal Judd-Ofelt Parameter and Radiative Properties of Sm^{3+} ions Doped Zinc Bismuth Borate Glasses", Opt. Mater, 32 (2009) 399.

[18] I Pal, A. Agarwal, S. Sanghi, M.P. Aggarwal. Structural, Absorption and Flurescence Spectral Analysis of Pr^{3+} ions Doped Zinc Bismuth Borate Glasses. Alloys Compds, 509 (2011) 7625.

[19] S. Sanghi, I. Pal, A. Agarwal, M.P. Aggarwal. Effect of Bi_2O_3 on Spectroscopic and Structural Properties of Er^{3+} Doped Cadmium Bismuth Borate Glasses, Spectro. Chema Acta 83 (2011) 94.

[20] M.J. Weber. Probabilities for radiative and nonradiative decay of Er^{3+} in LaF_3. Physical Review 157(2) (1967) 157.